Quaternary Research 84 (2015) 1–11

Contents lists available at ScienceDirect

Quaternary Research

journal homepage: www.elsevier.com/locate/yqres

Lake core record of Grinnell Glacier dynamics during the latest Pleistocene deglaciation and the Younger Dryas, Glacier National Park, Montana, USA

Nathan S. Schachtman [a,*], Kelly R. MacGregor [a], Amy Myrbo [b], Nora Rose Hencir [a], Catherine A. Riihimaki [c], Jeffrey T. Thole [a], Louisa I. Bradtmiller [d]

[a] Geology Department, Macalester College, Saint Paul, MN 55105, USA
[b] LacCore, University of Minnesota, Minneapolis, MN 55455, USA
[c] Council on Science and Technology, Princeton University, Princeton, NJ 08544, USA
[d] Department of Environmental Studies, Macalester College, Saint Paul, MN 55105, USA

ARTICLE INFO

Article history:
Received 3 October 2014
Available online 27 May 2015

Keywords:
Glacier National Park
Lake sediment core
Late Pleistocene
Holocene
Younger Dryas
Grinnell Glacier
Total inorganic carbon
Last Glacial Maximum
Glacial erosion
Geomorphic change

ABSTRACT

Few records in the alpine landscape of western North America document the geomorphic and glaciologic response to climate change during the Pleistocene–Holocene transition. While moraines can provide snapshots of glacier extent, high-resolution records of environmental response to the end of the Last Glacial Maximum, Younger Dryas cooling, and subsequent warming into the stable Holocene are rare. We describe the transition from the late Pleistocene to the Holocene using a ~17,000-yr sediment record from Swiftcurrent Lake in eastern Glacier National Park, MT, with a focus on the period from ~17 to 11 ka. Total organic and inorganic carbon, grain size, and carbon/nitrogen data provide evidence for glacial retreat from the late Pleistocene into the Holocene, with the exception of a well-constrained advance during the Younger Dryas from 12.75 to 11.5 ka. Increased detrital carbonate concentration in Swiftcurrent Lake sediment reflects enhanced glacial erosion and sediment transport, likely a result of a more proximal ice terminus position and a reduction in the number of alpine lakes acting as sediment sinks in the valley.

Introduction

Climate in the northern U.S. Rocky Mountains during the transition from the Last Glacial Maximum (LGM) to the Holocene is well constrained through modeling studies, terrestrial mapping of glacial deposits, and wetland and lake core records. Range-scale modeling studies suggest that following the LGM, the southern margins of the ice sheet retreated and summer insolation increased, resulting in warmer, drier summers along with wetter winters in the northern Rockies east of the Continental Divide (e.g., Bartlein et al., 1998). Terminal moraines recording individual glacier response to climate variability during the late Pleistocene to Holocene transition document a complex and non-uniform glacial retreat both locally and regionally. Terminal moraines in the northern Rocky Mountains date to between ~18.8 and 16.5 ka, while those in the Wind River Range have been shown to be significantly (~5 ka) younger (Gosse et al., 1995a; Licciardi et al., 2004; Licciardi and Pierce, 2008; Young et al., 2011). The variability in glacier behavior has been attributed to presence of the North American ice sheets, which affected the spatial and temporal pattern of moisture delivery to western U.S. glaciers, altering their mass balance characteristics (e.g. Licciardi et al., 2004; Thackray, 2008). However, limited regional records have hindered our ability to accurately characterize this non-uniform response to overall warming during this period, and more broadly glacier response to abrupt climate change in the late Pleistocene.

The Younger Dryas (YD) chronozone was a period of intense northern hemispheric cooling prior to climate stabilization of the Holocene (e.g., Alley, 2000; Muscheler et al., 2008). While data from the GISP2 ice core (Alley, 2000) defines the YD as occurring between 12.9 and 11.7 ka, more recent studies have suggested that the onset of the YD was later, between 12.8 and 12.75 ka (Wang et al., 2001; Muscheler et al., 2008). Terrestrial records of the YD (primarily moraines) in the North American Rocky Mountains demonstrate that glacial advances associated with the onset of cooler conditions occurred in areas such as Colorado and Wyoming (e.g., Reasoner et al., 1994; Gosse et al., 1995b; Menounos and Reasoner, 1997), but not in others (Clark and Gillespie, 1997). For example, Reasoner and others (1994) showed that deposition of the Crowfoot moraines in the Canadian Rockies might have been caused by the YD oscillation, indicating an onset and

* Corresponding author.
E-mail address: nathanschachtman@gmail.com (N.S. Schachtman).

http://dx.doi.org/10.1016/j.yqres.2015.05.004
0033-5894/

subsequent retreat of glaciers in the area, and Gosse and others (1995b) argued the Titcomb Lakes moraine in Wyoming was coincident with the YD cooling (moraines dated between 13.8 and 12.0 ka, with a mean of 12.7 ka (from a recalculated CRONUS age, Licciardi and Pierce, 2008)). MacLeod and others (2006) suggest that moraines nearest the margins of some modern glaciers in western Glacier National Park were likely coincident with the YD chronozone, supported by tephra ages and average lake sedimentation rates. While these records provide information on the instantaneous terminus positions of valley glaciers, both the timing of moraine development and the details of ice response to regional cooling are not well constrained. Constraining the glaciologic and geomorphic response of landscapes to the YD can provide insights into how complex alpine systems respond to abrupt hemispheric cooling events.

Lake sediment cores have been used to document ecological and environmental change, including the timing and pace of warming during the late Pleistocene and Holocene in the Rocky Mountains (e.g., Beiswenger, 1991; Whitlock, 1993; Mumma et al., 2012; Krause and Whitlock, 2013). These records are widespread in the northern Rocky Mountains of the U.S. and Canada, and come from a range of alpine, subalpine and lowland lake environments. Exposure-age chronologies from the Yellowstone Plateau indicate that glaciers had reached their LGM positions between 19 and 15 ka (Licciardi and Pierce, 2008) and evidence from a lake core in Glacier National Park, Montana (GNP) suggest that the major glacial retreat during the post-LGM deglaciation had occurred by 14 ka (Carrara, 1995). In addition, lacustrine records in the region show a distinct change from cool and dry vegetative conditions before ~17 ka to warmer and wetter vegetative conditions by ~11.5–10.5 ka (Whitlock, 1993; Mumma et al., 2012; Krause and Whitlock, 2013). Vegetation records from the northern Rockies do not characterize the YD cold interval as a full vegetation reversal; however, some records indicate a prolonged cool period following deglaciation and lasting until ~11.5 ka (Krause and Whitlock, 2013). Although the dates of glacier maximum positions are well constrained in the northern U.S. Rockies, precise timing of the advance and retreat of these glaciers is not well understood and has been shown to be spatially variable (Licciardi et al., 2004; Thackray, 2008).

Alpine glacier response to Holocene warming has been documented in many lacustrine records from the region (e.g., Leonard, 1997; Leonard and Reasoner, 1999; Munroe et al., 2012). Glacier activity exerts a first-order control over the character of sediment accumulating in downstream lakes, primarily as a result of subglacial erosion, sediment evacuation and proglacial transport (e.g., Karlén, 1981). Several studies have used varve thickness in alpine lakes as a proxy for summer temperature, as temperature offers a strong control on ablation rates, resulting in either enhanced subglacial erosion and/or more sediment entering the lake via melt water (Leonard, 1985; Loso et al., 2004). Leonard (1997) noted that at timescales of centuries to millennia, high sedimentation rates coincided with known periods of increased glacier extent, while at shorter time scales they were associated with transitional periods of glacier ice increase or decrease in ice-proximal lakes. Glacial fluctuations during the Holocene have also been identified through changing concentrations of mineral tracers (e.g. $CaCO_3$) in down-valley lake cores (Leonard and Reasoner, 1999; Munroe et al., 2012). While these ice-proximal records document the glacial geomorphic response to climate fluctuations during minor climate fluctuations such as the Little Ice Age (~AD 1400–AD 1850; Munroe et al., 2012), there are few investigations of lacustrine records in the northern Rocky Mountains that track glacier response during major climate shifts in the late Pleistocene and offer a well constrained record of the YD cooling. Building on previous research by MacGregor and others (2011) in the same field location, we use detrital dolomite, in concert with proxies for geomorphic processes and climate, to discern the timing of glacial response of the alpine valley in northwestern Montana during the late Pleistocene.

Field setting

The Many Glacier region of GNP is located east of the Continental Divide in northwestern Montana (Fig. 1). We analyzed the lowermost 3.19 m of a 9.25 m-long sediment core from the southern subbasin of Swiftcurrent Lake, the fourth in a chain of proglacial lakes down valley from Grinnell Glacier. Swiftcurrent Lake is 1.6 km long, ~0.5 km wide, and sits at an elevation of 1485 m. Bathymetric studies and additional lake cores show that the lake is split into two subbasins by a topographic drainage divide, each with a distinct depositional record. The northeastern basin of Swiftcurrent Lake drains approximately 44 km^2 and is primarily fed by Swiftcurrent Creek. The southwestern subbasin, where the core was collected, drains 36 km^2 and is dominated by meltwater inflow via Grinnell Creek from Grinnell Glacier to the southwest (MacGregor et al., 2011).

Steep hillslopes characterize the valley surrounding the lakes. Lake bathymetry and the surrounding topography suggest that the coring site, located at 8 m water depth, receives little if any sediment from Swiftcurrent Creek (MacGregor et al., 2011). The relief of the valley floor is low, with a ~50 m elevation change between lower Grinnell, Josephine and Swiftcurrent lakes. There is a ~460 m bedrock step that separates lower Grinnell Lake from Upper Grinnell Lake, which fills the cirque basin not covered by the modern Grinnell Glacier.

Swiftcurrent Valley, which incorporates Grinnell Glacier and drains into the southwestern subbasin of Swiftcurrent Lake via Grinnell Creek, is underlain by the Middle Proterozoic Belt Supergroup, comprised primarily of siltstones and argillites. Directly underlying Grinnell Glacier and the cirque basin is the Siyeh Limestone of the Helena Formation (Fig. 1). The Siyeh Limestone consists of dolomitic argillite (Whipple, 1992) and is the only known bedrock source of dolomite and calcite in the valley (MacGregor et al., 2011).

Methods

A series of overlapping cores were collected from a floating platform using square rod piston corers (Wright, 1967, 1991) during the summers of 2005 and 2010. Cores were logged for gamma density and magnetic susceptibility, then split, digitally photographed, and described at LacCore, University of Minnesota. The bottom 4 m were analyzed for L*a*b* color using color-corrected digital images (Balsam et al., 1999). Subsampling was conducted at 0.5–1 cm intervals from ~600–925 cm below the sediment-water interface in four separate core sections. Sample intervals were based on visual color differences, which became more apparent toward the bottom of the section, to keep each sample homogeneous in color (Fig. 2). The samples were analyzed for carbon/nitrogen (C/N), percent organic and inorganic carbon content (%TOC and %TIC), grain size, and mineralogy. Lead-210 analyses were conducted on bulk sediment at the St. Croix Watershed Research Station and modeled using the constant rate of supply (CRS) model (Appleby and Oldfield, 1978). Radiocarbon dates were obtained at Lawrence Livermore National Labs Center for Accelerator Mass Spectrometry from microscopic charcoal fragments or pollen concentrates prepared at LacCore. Analysis of the tephras encountered in the cores was conducted using a JEOL 6610LV scanning electron microscope with an Oxford Instruments energy dispersive X-ray spectrometer (SEM/EDS).

We used a Thermo Electron Flash Elemental Analyzer 1112 configured for analysis of C and N. Before analysis, samples were weighed and acidified with sulfurous acid to remove inorganic carbon, with an average sample size before acidification of 13.0 mg. For samples containing low amounts of carbon and nitrogen, sample size was increased fivefold. C/N analysis was limited to between every 2 and 4 cm throughout the core.

Total carbon analysis (%TC) was performed using a UIC CM5015 coulometer with a CM5200 auto-sampler furnace every 2 cm from ~550 to 600 cm and every centimeter in from 600 to 767 cm. Analysis of %TIC

https://doi.org/10.1016/j.yqres.2015.05.004 Published online by Cambridge University Press

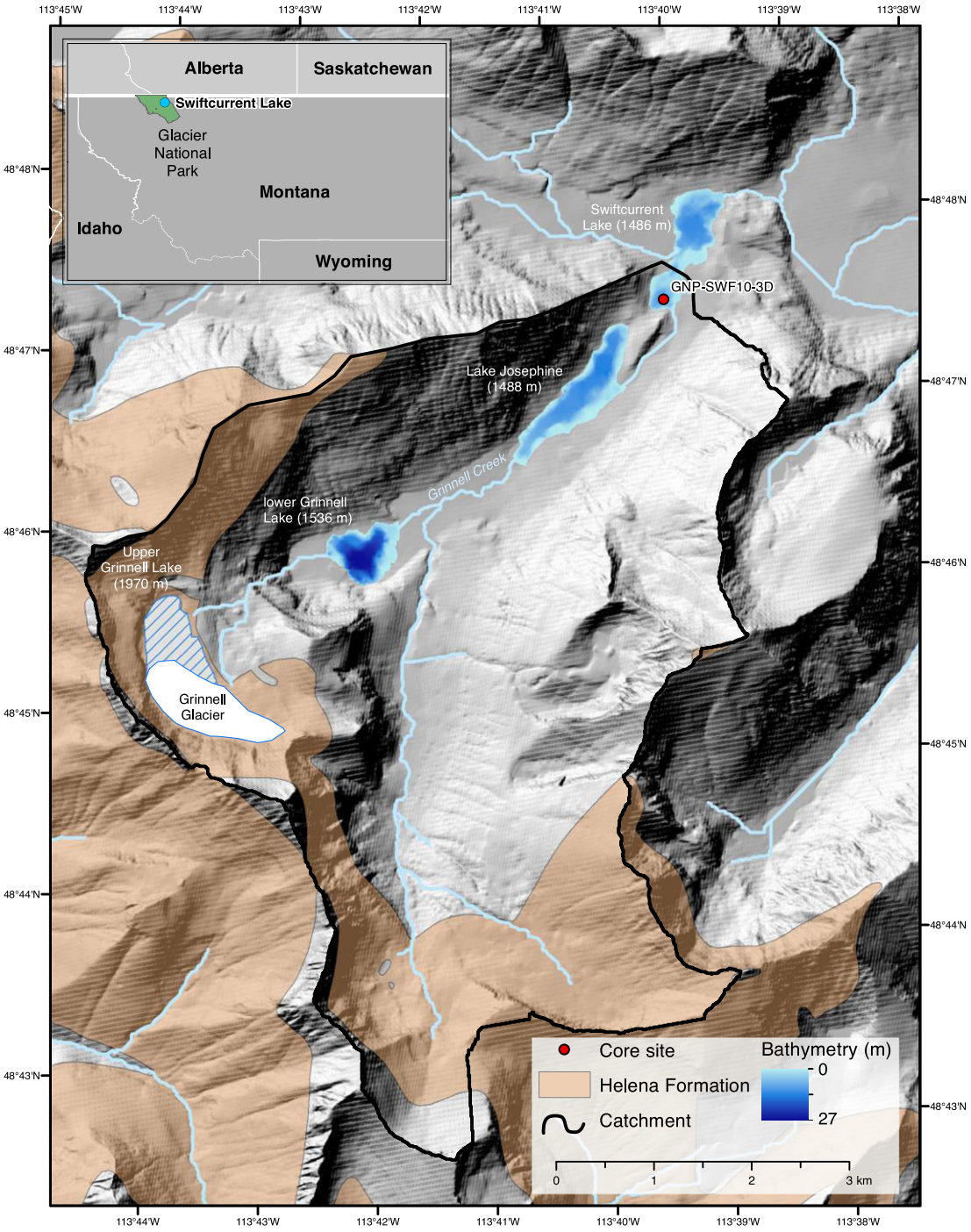

Figure 1. Site map of Glacier National Park, Montana (inset), with core location in Swiftcurrent Lake (red dot). Meltwater flows from Grinnell Glacier and Upper Grinnell Lake in the southwest through lower Grinnell Lake, Lake Josephine and Swiftcurrent Lake to northeast. The Helena Formation (brown) directly underlies Grinnell Glacier in the upper portion of the valley (Whipple, 1992). A topographic drainage divide at the narrowest part of Swiftcurrent Lake separates the body of water into two subbasins, the southwestern basin supplying the sediment at the coring site (black line).

was conducted using a CM5240 acidification module at the same intervals as %TC. Percent TOC was calculated by subtracting TIC from TC.

Grain size sampling was conducted at ~1–2 cm intervals, with analyses every other cm in the top ~60 cm and variable sampling according to color and texture changes in the bottom ~265 cm of core. Smear slide analysis revealed trace diatoms between depths of 540 and 593.5 cm and none below this depth, therefore rendering it unnecessary to pretreat our samples with NaOH. Samples were treated with H_2O_2 to remove organic matter, and analyses were performed on a Horiba LA-920 Grain Size Analyzer with a range of 0.2 μm–2 mm grain-size detection, assuming spherical quartz grains.

Mineral identification was performed on a PANalytical X'Pert Pro MPD X-ray diffractometer (XRD) every 2 cm from ~550 to 600 cm and almost every cm between ~600 and 767 cm. Semi-quantitative XRD analyses were performed every 4 cm using both the clay fraction approach and the normalized relative intensity ratio (RIR) method (Moore and Reynolds, 1997; Hiller, 2003). Quantitative uncertainties are low (1–2%) when minerals comprise 30–70% of a sample by volume

https://doi.org/10.1016/j.yqres.2015.05.004 Published online by Cambridge University Press

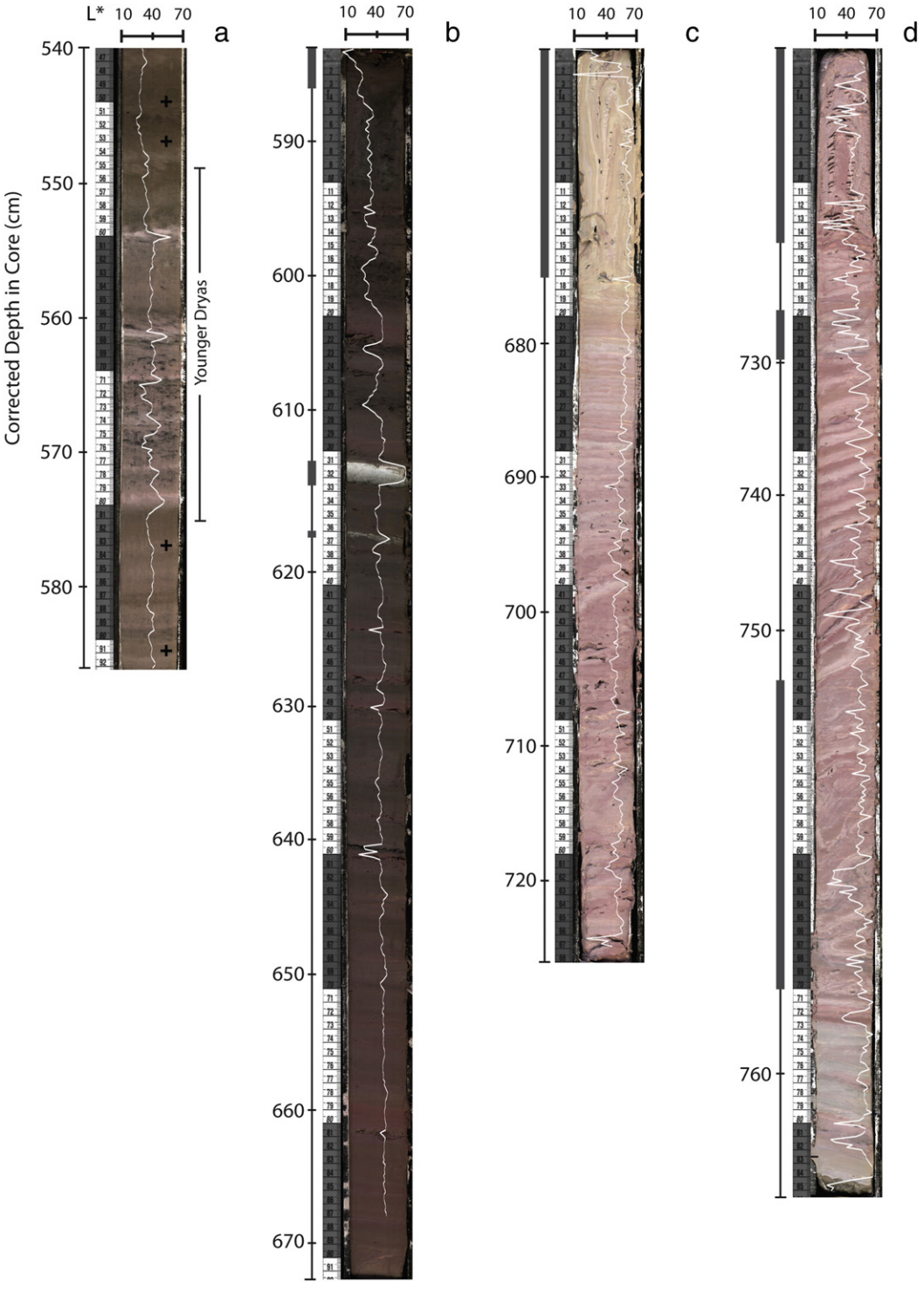

Figure 2. Image and color analysis of the four core sections from Swiftcurrent Lake, spanning 17 to 11.2 ka. The white line over each core image represents lightness (L*) in the CIE L*a*b* color space on the X-axis in each core image. Scale on the Y-axis in each image is cm with the cumulative, corrected depths in cm to the left of each core image. Areas shaded in gray were removed from our depth model (ie: tephras, slumped material). (a) 540–586 cm: Dominantly brown with fine laminations, similar to the cores from 0–540 cm (not shown); distinctive pink, brown, and black laminations from 55–81 cm were deposited during the Younger Dryas. (b) 586–672 cm: Predominantly brown color with pink bands increasing downcore. Glacier Peak G ash (30.8–32.5 cm) and Mt. St. Helens J ash 2.5 cm below appear as distinct white deposits. 0–3 cm is disturbed. (c) 672–725 cm: Core sediments predominantly pink in color reflecting increasing concentration of carbonate minerals. 0–17.5 cm is folded and interpreted as disturbed from piston suction during coring. (d) 725–767 cm Sediments are pink, becoming gray near core base. Color analysis, grain size, and stratigraphic constraints show couplets (interpreted as annual laminations) beginning at 23.5 cm. 0–14.5 cm is deformed from coring and 19.5 to 23.2 cm is removed due to folding.

and slightly higher (~7%) for very low (<15%) or very high (>85%) concentrations. The ratio of non-carbonate to carbonate was calculated assuming four end-member minerals: quartz, clays (e.g., illite), dolomite, and calcite.

Tephra units in GNP-SWF10-3D-6 L-1 (Fig. 2b), 2.5 cm and 0.5 cm thick were sampled and mounted in Buehler Konductomet, polished to 0.05 μm (alumina), and carbon coated. Both tephras were analyzed using a JEOL 6610LV Scanning Electron Microscope and an Oxford

https://doi.org/10.1016/j.yqres.2015.05.004 Published online by Cambridge University Press

Instruments X-Max 50 mm2 X-Max Energy Dispersive X-ray Spectrometer (SEM/EDS). The beam diameter was not measured, but an appropriate dead time was selected by spot size using a beam current of 0.70 nA for 30 s detector lifetime. Calibrations of element concentrations were conducted using Smithsonian Institute Microbeam Standards including both minerals and natural glasses. Based on pre- and post-standard analysis results, no corrections (other than normalizing to 100% volatile-free) were applied to the collected data. For each tephra, multiple shards (n = 24 and 32) were analyzed. Points that were either clearly minerals (Fe-rich or Al-rich) or had low analytical totals (e.g., <90%) were removed, as well as samples that had anomalously low SiO_2 concentrations. The remaining values were then normalized to 100 wt% on a dry basis for literature comparisons, and mean compositions for both tephras were calculated. We compared these data to existing datasets for western U.S. tephra using simple bivariate diagrams and a multivariate error-weighted similarity coefficient.

Results

Age-depth model

Overlapping cores correlated based on lithology from the sediment/water interface to a depth of ~7 m provide a high-quality depth model for sediment accumulation in Swiftcurrent Lake. Below this, we assume that the remaining two core sections have no gaps or re-cored sediment, based on visual inspection and observations in the field. The top of GNP-SWF10-3D-7 L-1 and GNP-SWF10-3D-8 L-1 are disturbed, likely as a result of suction from the Livingstone piston (Figs. 2c and d). We adjusted the reported depth of these two cores based on the thickness of laminations directly underlying the deformed material, the number of laminations observed in the deformed units, and depth of the drives. The thicknesses of three tephra layers, including a 48-cm thick Mazama ash, were removed from the depth model due to near — instantaneous deposition (e.g., MacGregor et al., 2011). A section of sediments that were visibly folded were assumed to be instantaneously deposited in a slump event and was also removed. The resulting composite depth of sediment is 7.67 m; here we focus on the oldest ~2.25 m.

The thickest tephra unit was identified as Mazama ash with a radiocarbon age of 7630 ± 150 cal yr BP (MacGregor et al., 2011, after Zdanowicz et al., 1999). Multivariate SIMAN calculations demonstrate that the middle tephra is the Glacier Peak G tephra (GP-G; SIMAN = 0.952), and the lower, thinner ash is Mount St. Helens J (MSH-J; SIMAN = 0.935). The tephras are distinct from each other (SIMAN = 0.878). SIMAN coefficients >0.95 indicate two tephras are most likely to be the same, while values 0.92–0.95 are likely similar but require further analysis, and <0.92 are unlikely to be related (Borchardt et al., 1972). The Glacier Peak G ash age is well constrained at 13,710–13,410 cal yr BP (Kuehn et al., 2009). We use 13,550 cal yr BP in our age model. There is less certainty regarding the age of MSH-J, in part due to several eruptions documented over the span of centuries at more proximal locations (e.g., Peterson et al., 2012). We utilize an age of 13,870 ± 100 cal yr BP, on the older end of the reported MSH-J estimate (Foit et al., 1993), in our age model for several reasons: (1) stratigraphically there is ~2.5 cm of laminated, fine-grained sediments between the tephras, which could represent several hundred years based on sedimentation rates above GP-G, (2) only one MSH-J ash was identified at Marias Pass, MT, located ~48 km (~30 miles) to the southeast from Swiftcurrent Lake (Carrara et al., 1986), suggesting that only one MSH eruption reached the region, and (3) the younger MSH-J ages reported by Peterson and others (2012) are from sites hundreds of km to the west of Glacier National Park, and the ages they report for the MSH-J ash would be stratigraphically above GP-G at our site.

In addition to tephra ages, 15 ^{210}Pb ages at the top of the core and eight calibrated ^{14}C ages throughout the core were used to construct the age-depth model. We assumed that the sediment-water interface dated to −60.5 yr (early July 2010). With the oldest datable horizon being the MSH-J tephra, we estimated a basal age for the core using a combination of two different sedimentation rates depending on whether core lithology (Fig. 2) indicated that the glacier was proximal to the lake (as in the lowest ~1 m of the composite core) or distal (as in the remainder of the composite core). Ice proximal sediments were interpreted as annual laminations (varves) based on macroscopic appearance, grain size, and CIE L*a*b* color analysis showing alternating colors in ~1 cm couplets. Couplets were assumed to represent one calendar year. For sediment that appeared disturbed (due to deformation during coring) and where the ice-proximal sediments are unlaminated and without cyclic color or grain size variations, we applied a linear sedimentation rate of 41 yr/cm, the average sedimentation rate between the GlPkG and MSH-J for lithologically similar sediments. Table 1 summarizes all dates used in the age-depth model. The Bayesian age-depth modeling program Bacon (Blaauw and Christén, 2011) was used to interpolate between dated horizons and assign ages to depths sampled for analysis (Fig. 3).

Lithology

Based on initial core descriptions, smear slide analysis, and grain size measurements, core material is dark gray to dark brown, massive to

Table 1
Age constraints and uncertainties in composite core.

Sample	Age (yr before 1950)	Age (^{14}C yr BP)	Error (yr)	Age (calibr. yr BP, 2-sigma)	Depth in core (cm)
SWI	−60.5		0.10		0.1
lead1	−60.4		1.47		0.25
lead2	−56.3		1.50		2.25
lead3	−49.1		1.65		4.25
lead4	−40.1		1.95		6.25
lead5	−28.7		2.27		8.25
lead6	−22.2		2.58		9.25
lead7	−16.6		2.72		10.25
lead8	−10.0		3.10		11.25
lead9	−2.0		3.88		12.25
lead10	15.0		4.17		14.25
lead11	33.2		4.25		16.25
lead12	57.1		7.57		18.25
lead13	92.1		9.52		20.25
lead14	111.7		16.16		21.25
lead15	131.9		28.72		22.25
CAMS-150349		1200	30	1250–1010	71
CAMS-153582		2800	30	2970–2800	189.5
CAMS-125098		3160	35	3450–3270	237.5
CAMS-124257		3945	35	4520–4260	309
Mazama tephra	7630		150		449
CAMS-153579		9950	40	11,600–11,250	544
CAMS-124258		9760	80	11,330–10,790	547
CAMS-153580		11,035	50	13,040–12,760	577
CAMS-153581		11,570	70	13,550–13,280	585
GlPkG tephra	13,550		150		614.05
MSHJ tephra	13,870		100		617.55
base_41_22.3	16,974		150		767.15

Samples and settings used in the Bacon age-depth model (Blaauw and Christén, 2011). "SWI" is the sediment-water interface; "lead(#)" are lead-210 dates from the St. Croix Watershed Research Station; "CAMS-" are radiocarbon dates on charcoal fragments or pollen concentrates from Lawrence Livermore National Laboratories Center for Accelerator Mass Spectrometry; "GlPkG" is the Glacier Peak G tephra; "MSHJ" is the Mount St. Helens J tephra; and "base_41_22.3" is the extrapolated date for the base of the core, using the rationale detailed in the text under "Age-depth model." Ages are given in either radiocarbon years BP (radiocarbon dates) or years before 1950 (SWI, lead-210, tephra, and basal dates); radiocarbon dates were calibrated using the IntCal13 curve (Reimer et al., 2013), with Calib 7.1 (for numerical 2-sigma ranges) and Bacon (for age-depth modeling). Errors for radiocarbon and lead-210 dates are lab errors, errors on tephra dates are estimated from the literature, and the error on the basal date is estimated. Additional Bacon settings include: acc.mean = 20, acc.shape = 1.5, mem.mean = 0.7, mem.strength = 4, and section thickness = 10 cm; reservoir age was considered to be 0; t.a = 3 for radiocarbon samples and 33 for others; t.b = 4 for radiocarbon samples and 34 for others. All settings, including t.a, and t.b, are as described in the Bacon 2.2 manual.

https://doi.org/10.1016/j.yqres.2015.05.004 Published online by Cambridge University Press

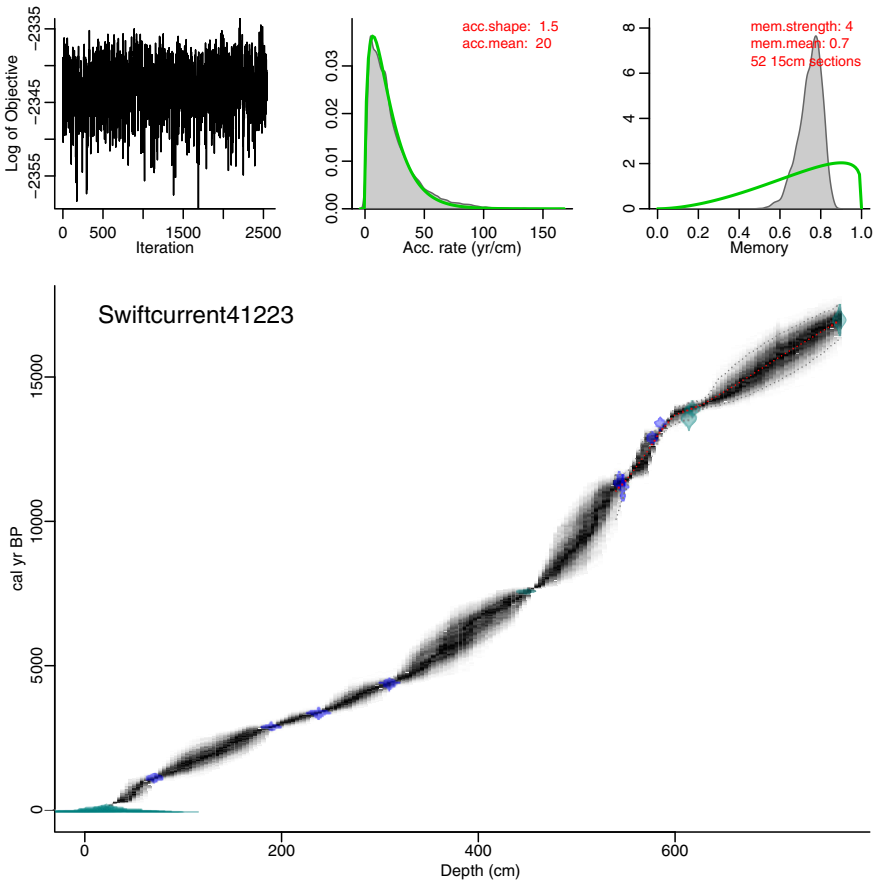

Figure 3. Bacon age-depth model based on eight radiocarbon, three tephra, and fifteen ^{210}Pb age constraints (Blaauw and Christén, 2011). 95% confidence intervals are shown by gray dots and the possible distribution is shown in gray shading. The densest shading indicates the most likely age. Note the narrow confidence intervals around the YD period from ~12.75 to 11.5 ka.

laminated silts and clays (Fig. 2). Between 550 and 575 cm, the sediment abruptly changes to a solid layer of thin brown, pink, and gray laminations ~1–2 cm in thickness, with less evidence of bioturbation or other disturbances (Fig. 2a). Smear slides taken from this layer show clay and silt with presence of amphibole, feldspars and dolomite. Sediment below ~625 cm is predominantly pink to pinkish-gray (Figs. 2b, c and d). Between ~690 and 725 distinct couplets 2–4 cm thick occur, distinguishable by grain size and color (Fig. 2c). Core density varies between 1.3 and 1.9 g/cm^3 and generally increases downcore.

Total organic carbon

Percent total organic carbon (%TOC) varies between 0 and 4%, remaining <1% between ~17 and 13.2 ka (Fig. 2, 767–585 cm), when values increase abruptly to ~2% (Fig. 4a). Percent TOC remains >1% between ~13.2 and 12.75 ka (585–572 cm), abruptly decreases to <1% between 12.75 and 11.5 ka (572–549 cm), and steadily increases between ~11.5 and 11.2 ka (572–549 cm) to values that characterize the relatively warm temperatures during the Holocene at Swiftcurrent Lake (MacGregor et al., 2011).

Total inorganic carbon

Percent TIC (%TIC) decreases during the period of record, from 5% at 17 ka to 0% starting at ~13.5 ka (Fig. 4b, 767–585 cm). There is no inorganic carbon present in the core between 13.5 and 12.75 ka (585–575 cm). Values increase to ~1% between 12.75 and 11.5 ka, which is higher than any point during the remainder of the Holocene (MacGregor et al., 2011).

C/N ratios

The ratio of organic carbon to nitrogen (C/N) varies between 2.6 and 81, with 95% of C/N ratios between 5 and 25. The highest C/N values are found in the oldest sediments; C/N values are most variable between ~17 and ~15 ka (767–675 cm), and stabilize after this time (Fig. 4c). With the exception of a coarse-grained layer at ~14.4 (Fig. 4; peak in C/N, grain size and %TIC, 645 cm) and a slight decrease between 12.75 and 11.8 ka (572–555 cm), C/N values increase steadily from ~15 to ~11.2 ka (675–540 cm). Measurements of C/N in modern plant samples in and around Swiftcurrent valley show lacustrine algae and aquatic rooted plants typically have C/N values <12, terrestrial leaf material ranges between 10 and 26, and terrestrial stems range from 35–60 (Anderson, 2014). This is consistent with previous work suggesting lacustrine algae and lake-sourced carbon has low C/N ratios, and terrestrial organic material has higher C/N values (Meyers, 1994).

Grain size

Mean grain size varies from 1.5 to 11 μm, with an average of 4 μm (very fine silt). There is no significant trend in grain size across the core, although the largest grain sizes are found between ~17 and 16 ka (Fig. 4d, 767–720 cm), and in the coarse silt layer found at 14.4 ka. We sampled these coarser layers based on color and apparent

https://doi.org/10.1016/j.yqres.2015.05.004 Published online by Cambridge University Press

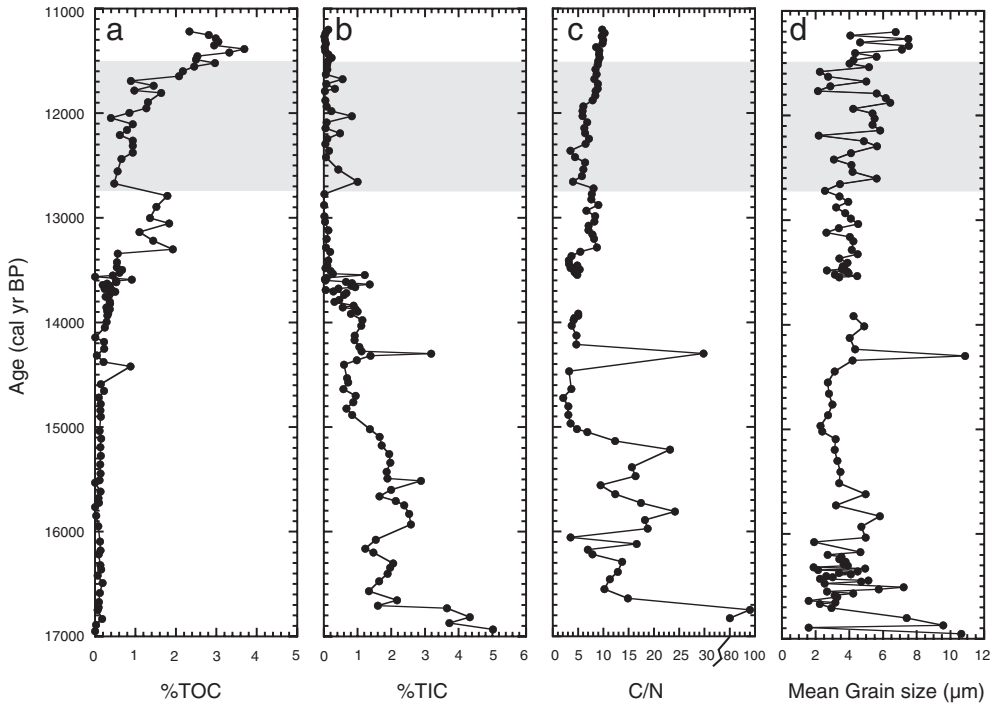

Figure 4. Swiftcurrent Lake core data from ~17 to ~11 ka; our proposed YD event indicated with gray bar. (a) Percent total organic carbon increases from 14.5–12.75 ka, drops and then increases through 11 ka. (b) Percent total inorganic carbon, reflecting authigenic dolomite and calcite deposition before ~14 ka and dolomite after ~14 ka. Percent TIC decreases from 17–14 ka, hovering near 0% until 11 ka except for slightly elevated values during the YD. (c) Ratio of mass percent organic carbon (C) to nitrogen (N). Ratios suggest primarily terrestrial organic contributions from 17–15 ka, with increasing algal sourcing between 15 and 11 ka. (d) Mean grain size, with data between ~17 and 16 ka supporting fine/coarse laminations indicative of varves. The spike in all data ~14.4 ka likely indicates a flood event.

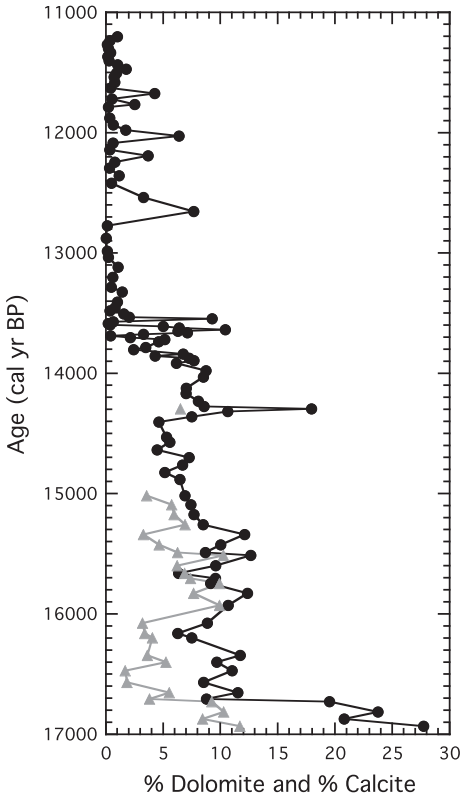

Figure 5. Percent dolomite (black line) and percent calcite (gray line) between 17 and 11 ka. Between 17 and 14.4 ka, the ratio of dolomite to calcite remains relatively constant, with dolomite being the dominant carbonate mineral.

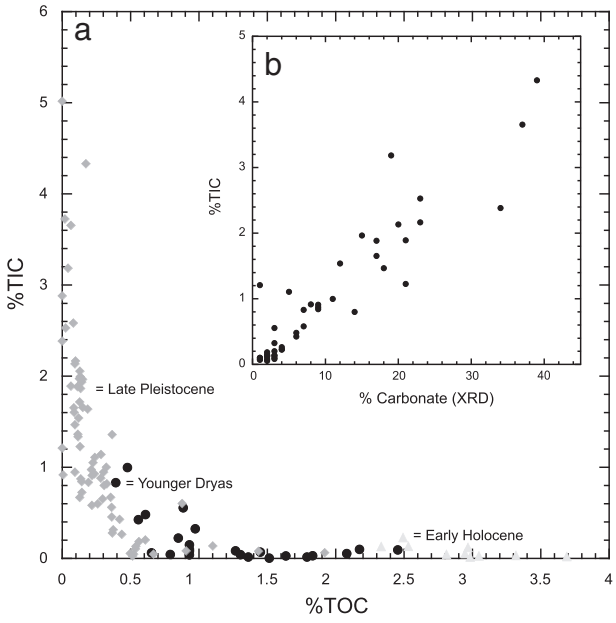

Figure 6. (a) Percent TIC vs. %TOC from ~17 to 11 ka at Swiftcurrent Lake. Values form distinct clusters that characterize the late Pleistocene (gray diamonds), Younger Dryas (black circles) and early Holocene (gray squares). (b) Percent TIC vs. % carbonate values from XRD. Linear relationship provides confirmation of our semi-quantitative XRD measurements. $R^2 = 0.87$.

https://doi.org/10.1016/j.yqres.2015.05.004 Published online by Cambridge University Press

density changes, discerning that darker layers correspond with larger grain sizes (6–10 μm) and the lighter layers constitute smaller grain sizes (<6 μm; Fig. 2d). With the exception of the period from ~17 to 16 ka with high %TIC and silt-sized grains, grain size does not follow trends in %TIC, suggesting that the grain size of all clastic sediments varies (Fig. 4d).

XRD mineralogy

Major minerals identified include quartz, dolomite, calcite, and trace amounts of clay minerals (MacGregor et al., 2011). Whereas quartz is the dominant mineral throughout the entire core, dolomite varies between 0 and 28% (Fig. 5). The relationship between %TIC and carbonate % minerals suggest that despite high uncertainties in semi-quantitative XRD analyses, carbonate % and %TIC are correlated (Fig. 6b). Calcite is always found in smaller amounts than dolomite, and follows the semi-quantitative abundance of dolomite. XRD data show both carbonate minerals are present between ~17 and 15 ka. Calcite does not appear in the core at any point between 14.4 ka and the present; dolomite was found in two additional windows during the Holocene (MacGregor et al., 2011; Figs. 5, 8). Non-carbonate to carbonate ratios are lowest at ~17 ka and increase at 13.8 ka (615 cm), as carbonate mineral abundance decreases to below detection (Fig. 7). Dolomite reappears and non-carbonate to carbonate ratios decrease for ~1200 yr between 12.5 and ~11.2 ka, when dolomite subsequently disappears from the record. Smear slide analysis shows dolomite grains are weathered and rounded, suggesting a detrital source, most likely from the Siyeh Limestone underlying Grinnell Glacier (MacGregor et al., 2011).

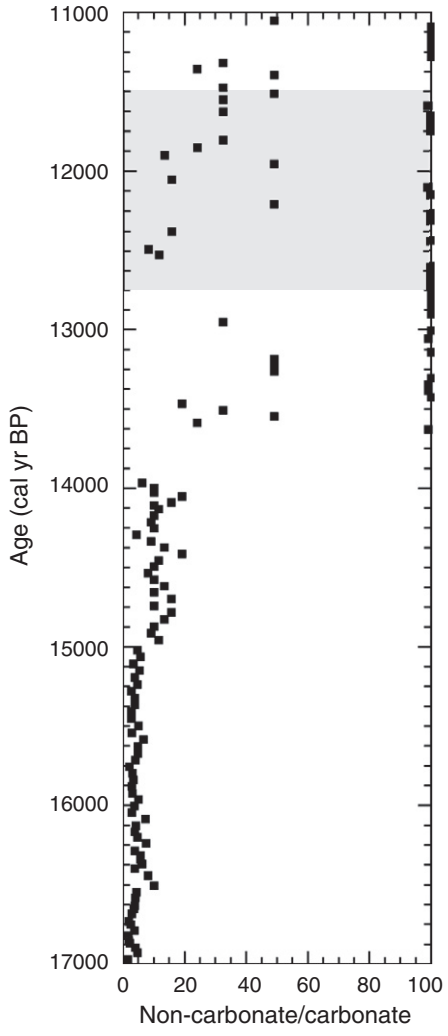

Figure 7. Ratio of non-carbonate minerals vs. carbonate (dolomite + calcite) percentage from XRD results between 17 and 11 ka. Our proposed Younger Dryas event is highlighted in gray. Quartz is the dominant mineral throughout the core. Maximum values of 100 indicate no carbonate present.

Discussion

Carbonate concentration as a proxy for glacial extent

Between 17 and 12.75 ka (Fig. 2, 767–575 cm), values of %TIC gradually decrease to below detection, while non-carbonate to carbonate ratios increase to 100, reflecting the increasing dominance of siliciclastic minerals (Figs. 4, 7). When carbonate is detected between 17 ka and present, dolomite is the dominant carbonate mineral observed in the Swiftcurrent Lake; calcite is only detected in the lake sediments between 17 and 14.4 ka and ratios of calcite to dolomite remain constant throughout this period (Fig. 5). We argue that greater amounts of detrital carbonate in Swiftcurrent Lake sediments indicate increased production and transport of primarily dolomite with small amounts of calcite from the Siyeh Formation. Based on its stratigraphic location in the valley, the detrital carbonates are likely being produced by Grinnell Glacier. Subglacial abrasion and headwall failures deliver this material to the proglacial environment, where it can be transported through the chain of lakes. Carbonate transport could be enhanced by increased hydrologic energy, or water discharge, through the lakes (e.g., MacGregor et al., 2011).

Grain size couplets are present in the core prior to ~15 ka (675 cm), where %TIC concentrations reach their highest levels at 5%. While we cannot directly correlate %TIC with glacier extent, higher %TIC likely indicates increased efficiency of transport of detrital carbonate from the valley head. Declining values of %TIC between ~17 and 13.5 ka (767–595 cm) suggest a retreating glacier, concurrent with northern hemisphere warming during this time. A small increase in %TIC values between 12.75 and 11.5 ka (575–549 cm) with a subsequent decrease to below detection at ~11.2 ka (540 cm) suggests a glacial advance, although not to the extent seen in late Pleistocene, and successive retreat into the warmer Holocene period. Lag time in the glaciologic response of Grinnell Glacier to abrupt cooling, as well as sediment transport down valley, could shift these intervals of glacial advance and retreat several hundred years older (e.g., Johannesson et al., 1989). Leonard (1997) suggests that on timescales of centuries to millennia, the highest sedimentation rates may be associated with glacier maximum stands. In Glacier National Park, increased carbonate flux in lakes downstream from glaciers has been observed during periods of known glacier advances, such as the Little Ice Age (1350 to 1850 AD; Munroe et al., 2012). This supports our interpretation that higher %TIC values are indicative of an expansive Grinnell Glacier in the valley, which could have intensified erosion of the underlying bedrock and increased down valley dolomite transport (MacGregor et al., 2011).

Carbonate presence coincides with periods of low %TOC values throughout the last 17 ka, indicating that detrital carbonate is transported and deposited under a suite of cooler, or more hydrologically energetic, conditions (Figs. 4, 7). However, %TOC values can also vary as a result of changing glacial sediment flux into alpine lakes. Intensified erosion, production and transport of glacially-derived sediment during periods of an extended glacier effectively decrease %TOC by dilution, and this relationship has been used as a proxy for glacigenic sediment flux in proglacial lakes (Karlén, 1976; Leonard, 1985, 1986, 1997). Between 17 and 11.2 ka at Swiftcurrent Lake, %TOC and %TIC values are anticorrelated, suggesting that %TOC may reflect changing inputs of %TIC into Swiftcurrent Lake, effectively producing a swamping signal (Fig. 6a). This relationship does not hold true from 11.2 ka to the present; previous work demonstrates

https://doi.org/10.1016/j.yqres.2015.05.004 Published online by Cambridge University Press

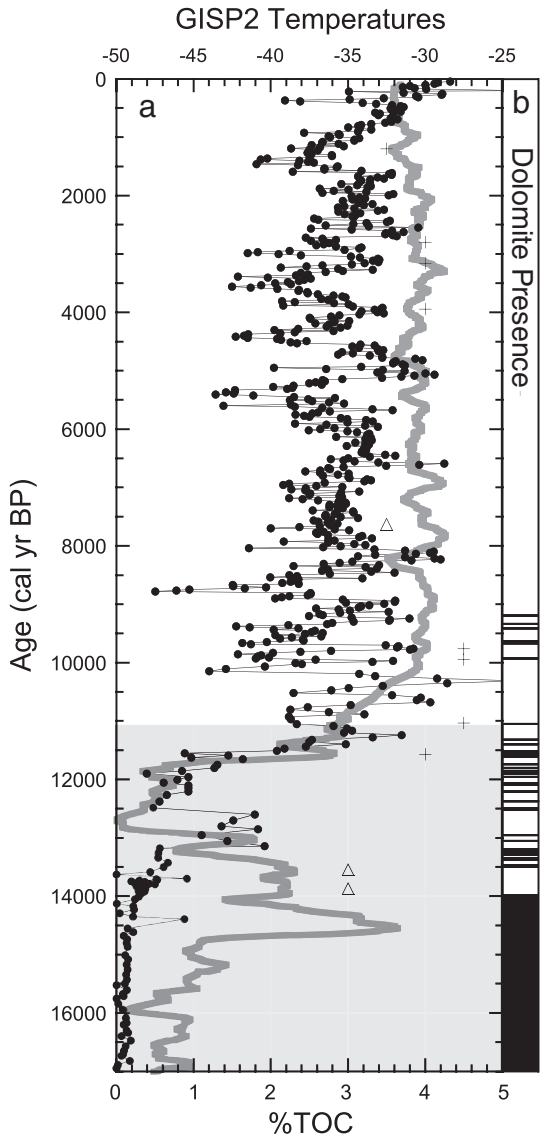

Figure 8. (a) Percent TOC (black line), GISP2 temperatures (gray line) and (b) dolomite presence from 17 ka–present (Alley, 2000; MacGregor et al., 2011;). Radiocarbon ages (crosses) and tephra units (triangles) are also shown.

that %TOC values are linked to solar forcing since ~7.6 ka. We suggest organic input, not clastic sediment flux, is the major control on %TOC after ~11.2 ka (MacGregor et al., 2011; Fig. 8). Regardless of whether %TOC values at Swiftcurrent Lake are indicative of organic carbon production or a signal of changing glacial sediment flux, we interpret periods of low %TOC as reflecting cooler conditions in the valley, associated with an expanded glacier (Fig. 6a).

Late Pleistocene environmental conditions (~17–12.75 ka; 767–575 cm)

Low %TOC and decreasing %TIC, C/N, and grain size characterize the late Pleistocene, implying gradual glacier retreat. We interpret this as reflecting climatic warming from cool conditions at Swiftcurrent Lake. A gradual decline in %TIC values from 17 to 12.75 ka provides evidence for a diminished footprint of Grinnell Glacier, and a decrease in mean grain size suggests an increasingly distal source of sediment, possibly associated with glacial retreat and exposure of additional lacustrine sinks in the valley. An overall decrease in C/N values indicates a shift away from terrestrial organic material and to algal sourcing of organic matter (Meyers, 1994). Abrupt increases in %TOC and C/N values ca. ~13.2 ka (585 cm) suggest rapid warming with increased availability of terrestrial organic matter or decreased %TIC transport to the lake. Glacial retreat and warmer temperatures as inferred from our record between ~17 and 12.75 ka are consistent with modeled increases in summer insolation during this time, which caused increased summer temperatures and decreased summer effective moisture (Bartlein et al., 1998). Areas proximal to receding glaciers, such as Swiftcurrent valley, may have not experienced the dry conditions seen elsewhere in the western U.S. immediately following the warming pulse.

Our observations are consistent with other lacustrine records of climate change in the northern Rocky Mountains (e.g., Carrara, 1995; Brunelle and Whitlock, 2003; Mumma et al., 2012). In southern Montana, ~403 km (~250 miles) south of the study area, a gradual shift from alpine tundra to subalpine parkland and warmer conditions has been documented, beginning at ~17 ka (Mumma et al., 2012). Approximately 322 km (200 miles) to the southwest at Burnt Knob Lake in Northern Idaho, an expansion of subalpine taxa (Picea and Abies) at ~14 ka was documented, indicating a shift to warmer summer temperatures at that time (Brunelle and Whitlock, 2003). Increases in %TOC at Swiftcurrent Lake correspond with this documented regional warming ~14 ka, as well as with previous work ~32 km (~20 miles) south of the study area suggesting that re-growth following regional deglaciation in the GNP area occurred before 12.2 ka (Carrara, 1995).

Younger Dryas (12.75–11.5 ka; 575–549 cm)

In addition to the abrupt lithological changes described above, we interpret the abrupt decreases in %TOC and C/N and an increase in %TIC ~12.75 ka as marking the start of the YD in Swiftcurrent valley (Fig. 4). At Swiftcurrent Lake, coincident decreases in %TOC and C/N starting at 12.75 ka and ending at 11.5 ka indicate reduced organic matter in the lake. Decreased terrestrial carbon inputs, rather than an increase in algal carbon production, is likely the driver for the C/N decrease at 12.75 ka. Correlative with these increases is an abrupt spike in %TIC, increasing at 12.75 ka from ~0 to ~2% (Fig. 4). The reappearance of carbonates and a decrease in non-carbonate: carbonate may signal an increased Grinnell Glacier footprint in response to regional YD cooling.

Mean grain size is variable between 12.75 and 11.6 ka. While we might expect a decrease in grain size as a result of increased glacial flour flux during the YD, rapid advance and retreat of Grinnell Glacier could have contributed to unstable periglacial geomorphic conditions on the slopes of the valley. The melting of large masses of ice and coincident uncovering hillslopes with limited vegetative cover could have increased transport of coarser-grained clastic material into Swiftcurrent Lake.

Terminal moraines and pollen records from North America suggest the YD lasted from 12.9 to 11.7 ka (e.g., Reasoner and Jodry, 2000; Briles et al., 2012). Our observations are consistent with other studies of minor glacial advances during the YD in the northern Rocky Mountains, which date terminal moraines from the advance within this interval (Reasoner et al., 1994; Gosse et al., 1995b; Reasoner and Jodry, 2000; Beierle et al., 2003). However, few lake core records in the Rockies are analyzed with high enough resolution to characterize the YD event (e.g., Mumma et al., 2012; Krause and Whitlock, 2013). A notable exception is Doerner and Carrara (2001) who observe a decrease in organic sedimentation at McCall Fen in Idaho (12.7 and 12.2 ka) Our mean modeled age for the YD onset in Swiftcurrent valley of 12.75 ka is broadly consistent with other regional records of climate change and we note the age-depth model provides a 2-σ age between 12,397 and 13,023 cal yr BP (Fig. 3). As there are no moraines in the valley that would indicate the thickness or length of a late Pleistocene Grinnell Glacier, estimating response time of the glacier to a new steady-state condition following rapid cooling is not

https://doi.org/10.1016/j.yqres.2015.05.004 Published online by Cambridge University Press

realistic. It is possible that the glacial geomorphic response of Grinnell Glacier occurred slightly later and for a shorter duration in Grinnell Valley than records farther south, but our age-model uncertainties at 12.75 ka are large enough that the timing of onset may be coincident with the 12.7–12.9 ka onset observed elsewhere in the Rockies (Reasoner et al., 1994; Reasoner and Jodry, 2000; Doerner and Carrara, 2001).

Early Holocene (11.5 ka–11.2 ka; 549–540 cm)

Following the termination of the YD ~11.5 ka at Swiftcurrent Lake, there is an increase in %TOC and C/N, indicating an increase in temperature and enhanced terrestrial sourcing of organic matter to the lake. Percent TIC decreases to below detection at 11.5 ka, implying a diminished Grinnell Glacier footprint. Depending on how far Grinnell Glacier advanced down valley during the YD, its retreat would have exposed additional lakes in the chain, increasing the number and volume of potential sediment sinks up valley from Swiftcurrent Lake. Uncovering of additional sediment sinks, such as Lake Josephine, could immediately trap carbonate traveling through the hydrologic system and result in significantly less material deposited in Lake Swiftcurrent.

Our data from Swiftcurrent Lake are consistent with climate models and regional paleoclimate proxy records for the western U.S. during the Pleistocene/Holocene transition. Modeling simulations for this region between ~16 and 11 ka include the direct and indirect effects of variations in the seasonality of insolation. Increasing temperatures and decreasing effective moisture relative to full-glacial conditions are some of the direct effects, while indirect effects include warm dry summers resulting from the strengthening of the northeast Pacific subtropical high-pressure system (Bartlein et al., 1998). There is supporting evidence for warming in other parts of the northern Rocky Mountains during this period. Upslope migration of the tree line and increased fire frequency ~11 ka at Burnt Knob Lake indicate a shift to warmer and drier summers (Brunelle and Whitlock, 2003). Pollen records from the Rocky Mountains document a transition from alpine to subalpine species at 11.5 ka, suggesting a regional warming of climate at this time (Beiswenger, 1991; Whitlock, 1993; Mensing et al., 2012).

Comparison with the entire Holocene lacustrine record at Swiftcurrent Lake shows that %TOC increased at 11.3 ka and stabilized during the relatively warm Holocene period, concurrent with GISP2 temperature stabilization (MacGregor et al., 2011; Fig. 8). Throughout the Holocene, dolomite occurs in a few brief windows of time but not to the extent observed in the late Pleistocene (MacGregor et al., 2011; Fig. 8). Dolomite is not present during the Little Ice Age in the Swiftcurrent core, a time when photographic evidence demonstrates that Grinnell Glacier filled its cirque basin and removed Upper Grinnell Lake as a downstream sediment sink (Anderson, H.A., personal communication, 2014). This suggests either Grinnell Glacier must extend over the valley step to lower Grinnell Lake for dolomite to be transported to Swiftcurrent Lake, or that the hydrologic energy at the time is insufficient to move glacially produced sediment through at least two lake basins (i.e., lower Grinnell and Josephine). The scarcity of dolomite in the Swiftcurrent record during the past ~11 ka suggests that glacial activity was at a minimum when compared to the late Pleistocene and YD; this is consistent with records of climate and temperature variability during the Holocene. When compared to measurements and models of North American climate since the LGM, the complete record of dolomite presence from 17 ka to present at Swiftcurrent Lake supports our interpretation of dolomite minerals as a proxy for Grinnell Glacier activity.

Conclusions

A high-resolution lacustrine sediment core from Swiftcurrent Lake reflects the geomorphic and environmental response to climate change during the late Pleistocene-early Holocene in Glacier National Park, Montana. Broadly supported by other paleoclimate records in the northern Rocky Mountains, evidence from multiple proxies details a period of gradual glacial retreat between ~17 and 12.75 ka. An abrupt increase in %TIC, which reflects glacier size in the valley, and a decrease in %TOC and C/N at 12.75 ka reflect the glacial geomorphic and hillslope response to abrupt cooling in the valley, coeval with the Younger Dryas chronozone. The termination of the YD at 11.5 ka in Swiftcurrent valley is identical to other regional records; however, its lagged onset indicates that the YD was shorter in duration in the Swiftcurrent Lake region than in other areas in the northern Rocky Mountains. This suggests either a longer response time of Grinnell Glacier to abrupt cooling, possibly resulting from valley morphology, or a lagged onset of YD climate change in the northern U.S. Rocky Mountains. Glacially derived detrital carbonate, in concert with other geomorphic and climate proxies, can be used to trace glacier advance and retreat in this system. While we interpret %TIC as a proxy for the size and geomorphic footprint of Grinnell Glacier, this relationship becomes increasingly complicated by the presence of up to three intermediate hydrologic sinks. Investigating the temporally variable relationship between glacial erosion, sediment transport, and lake sedimentation during periods of glacial advance and retreat will yield additional constraints on the interpretation of both climate and geomorphic proxies in high alpine, ice proximal environments. The use of detrital sediment as an indicator of geomorphic source may help constrain climatic and concomitant geomorphic change in complex and changing landscapes.

Acknowledgments

We thank the Keck Foundation and NSF for supporting core collection as well as the Macalester College Wallace Faculty Research fund for providing financial support. We thank the LacCore facility (NSF-EAR-0949962) and staff for their support in the field and lab. Thanks to the National Park Service and the Glacier Park Boat Company for logistical support, and Kevin Theissen, St. Thomas University, for use of his Elemental Analyzer. Special thanks to Lucy Andrews and Jason Addison for their input and laboratory work in the tephra identification process. We are grateful to Doug Clark and Eric Leonard for helpful comments that significantly improved the manuscript.

References

Alley, R., 2000. The Younger Dryas cold interval as viewed from central Greenland. Quaternary Science Reviews 19, 213–226.
Anderson, H., 2014. High resolution lacustrine records of historical environmental change in Glacier National Park, Montana, U.S.A. Geology Honors Projects. Paper 15 (http://digitalcommons.macalester.edu/geology_honors/15).
Appleby, P.G., Oldfield, F., 1978. The calculation of lead-210 dates assuming a constant rate of supply of unsupported 210 Pb to the sediment. Catena 5 (1), 1–8.
Balsam, W.L., Deaton, B.C., Damuth, J.E., 1999. Evaluating optical lightness as a proxy for carbonate content in marine sediment cores. Marine Geology 161, 141–153.
Bartlein, P.J., Anderson, P.M., Anderson, K.H., Edwards, M.E., Mock, C.M., Thompson, R.S., Webb, R.S., Webb III, T., Whitlock, C., 1998. Paleoclimate simulations for North America over the past 21,000 years: features of the simulated climate and comparisons with paleoenvironmental data. Quaternary Science Reviews 17, 549–585.
Beierle, B.D., Smith, D.G., Hills, L.V., 2003. Late Quaternary glacial and environmental history of the Burstall Pass Area, Kananaskis Country, Alberta, Canada. Arctic, Antarctic, and Alpine Research 35, 391–398.
Beiswenger, J.M., 1991. Late Quaternary vegetational history of Grays Lake, Idaho. Ecological Monographs 61, 165–182.
Blaauw, M., Christén, J.A., 2011. Flexible paleoclimate age-depth models using an autoregressive gamma process. Bayesian Analysis 6, 457–474.
Borchardt, G.A., Aruscavage, P.J., Millard Jr., H.T., 1972. Correlation of Bishop Ash, a Pleistocene marker bed, using instrumental neutron activation analysis. Journal of Sedimentary Petrology 42, 301–306.
Briles, C.E., Whitlock, C., Meltzer, D.J., 2012. Last glacial–interglacial environments in the southern Rocky Mountains, USA and implications for Younger Dryas-age human occupation. Quaternary Research 77, 96–103.
Brunelle, A., Whitlock, C., 2003. Postglacial fire, vegetation, and climate history in the Clearwater Range, Northern Idaho, USA. Quaternary Research 60, 307–318.
Carrara, P.E., 1995. A 12 000 year radiocarbon date of deglaciation from the Continental Divide of northwestern Montana. Canadian Journal of Earth Sciences 32, 1303–1307.
Carrara, P.E., Short, S.K., Wilcox, R.E., 1986. Deglaciation of the mountainous region of northwestern Montana, U.S.A., as indicated by late Pleistocene ashes. Arctic and Alpine Research 18, 317–325.

Clark, D.H., Gillespie, A.R., 1997. Timing and significance of the Late-Glacial and Holocene Cirque Glaciation in the Sierra Nevada, California. Quaternary International 38–39, 21–38.
Doerner, J.P., Carrara, P.E., 2001. Late Quaternary vegetation and climatic history of the Long Valley Area, west-central Idaho, U.S.A. Quaternary Research 56, 103–111.
Foit, J.F.F., Mehringer, J.P.J., Sheppard, J.C., 1993. Age, distribution, and stratigraphy of Glacier Peak tephra in eastern Washington and western Montana, United States. Canadian Journal of Earth Sciences 30, 535–552.
Gosse, J.C., Evenson, E.G., Klein, J., Lawn, B., Middleton, R., 1995a. Precise cosmogenic ^{10}Be measurements in western North America: support for a global Younger Dryas cooling event. Geology 23, 877–880.
Gosse, J.C., Klein, J., Evenson, E.B., Lawn, B., Middleton, R., 1995b. Beryllium-10 dating of the duration and retreat of the last Pinedale glacial sequence. Science 268, 1329–1333.
Hiller, S., 2003. Quantitative analysis of clay and other minerals in sandstones by x-ray powder diffraction (XRPD). In: Worden, R.H., Morad, S. (Eds.), Clay Mineral Cements in Sandstones: Special Publication 34 of the International Association of Sedimentologists, pp. 213–251.
Johannesson, T., Raymond, C.F., Waddington, E.D., 1989. A simple method for determining the response time of glaciers. In: Oerlemans, J., Bentley, C.R. (Eds.), Glacier Fluctuations and Climatic Change. Kluwer Academic Publishing, Oerlemans.
Karlén, W., 1976. Lacustrine sediment and tree-limit variations as evidence of Holocene climatic fluctuations in Lappland, northern Sweden. Geografiska Annaler 58A, 1–34.
Karlén, W., 1981. Lacustrine sediment studies; a technique to obtain a continuous record of Holocene glacier variations. Geografiska Annaler: Series A: Physical Geography 63, 273–281.
Krause, T.R., Whitlock, C., 2013. Climate and vegetation change during the late glacial/early-Holocene transition inferred from multiple proxy records from Blacktail Pond, Yellowstone National Park, USA. Quaternary Research 79, 391–402.
Kuehn, S.C., Froese, D.G., Carrara, P.E., Foit, F.F., Pearce, N.J.G., Rotheisler, P., 2009. Major- and trace-element characterization, expanded distribution, and a new chronology for the latest Pleistocene Glacier Peak tephras in western North America. Quaternary Research 71, 201–216.
Leonard, E.M., 1985. Glaciological and climatic controls on lake sedimentation, Canadian Rocky Mountains. Zeitschrift Für Gletscherkunde Und Glazialgeologie 21, 35–42.
Leonard, E.M., 1986. Use of lacustrine sedimentary sequences as indicators of Holocene glacial history, Banff National Park, Alberta, Canada. Quaternary Research 26, 218–231.
Leonard, E.M., 1997. The relationship between glacial activity and sediment production; evidence from a 4450-year varve record of neoglacial sedimentation in Hector Lake, Alberta, Canada. Journal of Paleolimnology 17, 319–330.
Leonard, E., Reasoner, M., 1999. A continuous Holocene Glacial Record inferred from Proglacial Lake Sediments in Banff National Park, Alberta, Canada. Quaternary Research 51, 1–13.
Licciardi, J.M., Pierce, K.R., 2008. Cosmogenic exposure-age chronologies of Pinedale and Bull Lake glaciations in greater Yellowstone and the Teton Range, USA. Quaternary Science Reviews 27, 814–831.
Licciardi, J.M., Clark, P.U., Brook, E.J., Elmore, D., Sharma, P., 2004. Variable responses of western U.S. glaciers during the last deglaciation. Geology 32, 81–84.
Loso, M.G., Anderson, R.S., Anderson, S.P., 2004. Post-Little Ice Age record of coarse and fine clastic sedimentation in an Alaskan proglacial lake. Geology 32, 1065–1068.
MacGregor, K.R., Riihimaki, C.A., Myrbo, A., Shapley, M.D., Jankowski, K., 2011. Geomorphic and climatic change over the past 12,900 yr at Swiftcurrent Lake, Glacier National Park, Montana, USA. Quaternary Research 75, 80–90.
MacLeod, D.M., Osborn, G., Spooner, I., 2006. A record of post-glacial morainedeposition and tephra stratigraphy from Otokomi Lake, Rose Basin, Glacier National Park, Montana. Canadian Journal of Earth Sciences 43, 447–460.
Menounos, B., Reasoner, M.A., 1997. Evidence for Cirque Glaciation in the Colorado Front Range during the Younger Dryas Chronozone. Quaternary Research 48, 38–47.
Mensing, S., Korfmacher, J., Musselman, R., Minckley, T., 2012. A 15,000 year record of vegetation and climate change from a treeline lake in the Rocky Mountains, Wyoming, USA. Holocene 22, 739–748.
Meyers, P.A., 1994. Preservation of elemental and isotopic source identification of sedimentary organic matter. Chemical Geology 114, 289–302.
Moore, D.M., Reynolds Jr., R.C., 1997. X-Ray Diffraction and the Identification and Analysis of Clay Minerals 2nd ed. Oxford University Press, New York (378 pp.).
Mumma, S.A., Whitlock, C., Pierce, K.L., 2012. A 28,000 year history of vegetation and climate from Lower Red Rock Lake, Centennial Valley, southwestern Montana. Palaeogeography, Palaeoclimatology, Palaeoecology 326–328, 30–41.
Munroe, J.S., Crocker, T.A., Giesche, A.M., Rahlson, L.E., Duran, L.T., Bigl, M.F., Laabs, B.J.C., 2012. A lacustrine-based Neoglacial record for Glacier National Park, Montana, USA. Quaternary Science Reviews 53, 39–54.
Muscheler, R., Kromer, B., Björck, S., Svensson, A., Friedrich, M., Kaiser, K.F., Southon, J., 2008. Tree rings and ice cores reveal ^{14}C calibration uncertainties during the Younger Dryas. Nature Geoscience 1, 263–267.
Peterson, C.D., Minor, R., Gates, E.B., Vanderburgh, S., Carlisle, K., 2012. Correlation of tephra marker beds in latest Pleistocene and Holocene fill of the submerged lower Columbia River Valley, Washington and Oregon, U.S.A. Journal of Coastal Research 28, 1362–1380.
Reasoner, M.A., Jodry, M.A., 2000. Rapid response of alpine timberline vegetation to the Younger Dryas climate oscillation in the Colorado Rocky Mountains, USA. Geology 28, 51–54.
Reasoner, M.A., Osborn, G., Rutter, N.W., 1994. Age of the Crowfoot advance in the Canadian Rocky Mountains: a glacial event coeval with the Younger Dryas oscillation. Geology 22, 439–442.
Reimer, P.J., Bard, E., Bayliss, A., Beck, J.W., Blackwell, P.G., Ramsey, C.B., Buck, C.E., Cheng, H., Edwards, R.L., Friedrich, M., Grootes, P.M., Guilderson, T.P., Haflidason, H., Hajdas, I., Hatté, C., Heaton, T.J., Hoffmann, D.L., Hogg, A.G., Hughen, K.A., Kaiser, K.F., Kromer, B., Manning, S.W., Niu, M., Reimer, R.W., Richards, D.A., Scott, E.M., Southon, J.R., Staff, R.A., Turney, C.S.M., van der Plicht, J., 2013. IntCal13 and Marine13 Radiocarbon age calibration curves 0-50,000 years cal BP. Radiocarbon 55, 1869–1887.
Thackray, G.D., 2008. Varied climatic and topographic influences on Late Pleistocene mountain glaciation in the western United States. Journal of Quaternary Science 23, 671–681.
Wang, Y.J., Cheng, H., Edwards, R.L., An, Z.S., Wu, J.Y., Shen, C.C., Dorale, J.A., 2001. A high resolution absolute-dated Late Pleistocene monsoon record from Hulu Cave, China. Science 294, 2345–2348.
Whipple, J.W., 1992. Geologic map of Glacier National Park, Montana.1:100,000.
Whitlock, C., 1993. Postglacial vegetation and climate of Grand Teton and Southern Yellowstone National Parks. Ecological Monographs 63, 173–198.
Wright Jr., H.E., 1967. A square-rod piston sampler for lake sediments. Journal of Sedimentary Petrology 37, 975–976.
Wright Jr., H.E., 1991. Coring tips. Journal of Paleolimnology 6, 37–49.
Young, N.E., Briner, J.P., Leonard, E.M., Licciardi, J.M., Lee, K., 2011. Assessing climatic and nonclimatic forcing of Pinedale glaciation and deglaciation in the western United States. Geology 39, 171–174.
Zdanowicz, C.M., Zielinski, G.A., Germani, M.S., 1999. Mount Mazama eruption; calendrical age verified and atmospheric impact assessed. Geology 27, 621–624.

https://doi.org/10.1016/j.yqres.2015.05.004 Published online by Cambridge University Press